2012

UDP-glucose Dehydrogenase Polymorphisms from Patients with Congenital Heart Valve Defects Disrupt Enzyme Stability and Quaternary Assembly

Annastasia S. Hyde
University of Nebraska-Lincoln

Erin L. Farmer
University of Nebraska-Lincoln

Katherine E. Easley
University of Nebraska-Lincoln

Kristy van Lammeren
ubrecht Institute, Royal Netherlands Academy of Arts and Sciences (KNAW)

Vincent M. Christoffels
University of Amsterdam

See next page for additional authors

THE JOURNAL OF BIOLOGICAL CHEMISTRY VOL. 287, NO. 39, pp. 32708–32716, September 21, 2012

UDP-glucose Dehydrogenase Polymorphisms from Patients with Congenital Heart Valve Defects Disrupt Enzyme Stability and Quaternary Assembly*[S]

Received for publication, June 26, 2012 Published, JBC Papers in Press, July 18, 2012, DOI 10.1074/jbc.M112.395202

Annastasia S. Hyde[‡], Erin L. Farmer[‡], Katherine E. Easley[‡], Kristy van Lammeren[§], Vincent M. Christoffels[¶], Joseph J. Barycki[‡], Jeroen Bakkers[§1], and Melanie A. Simpson[‡2]

From the [‡]Department of Biochemistry, University of Nebraska, Lincoln, Nebraska 68588-0664, the [§]Hubrecht Institute, Royal Netherlands Academy of Arts and Sciences (KNAW), and University Medical Center Utrecht, 3584 CT Utrecht, The Netherlands, and the [¶]Department of Anatomy, Embryology and Physiology, Heart Failure Research Center, Academic Medical Center, University of Amsterdam, 1105 AZ Amsterdam, The Netherlands

Background: UDP-glucose dehydrogenase (UGDH) polymorphisms were identified in a screen of candidate genes for heart valve defects.
Results: Two individual mutants fail to rescue cardiac valve defects in UGDH-deleted zebrafish and have reduced stability *in vitro*.
Conclusion: UGDH loss of function mutations result in a subset of human congenital cardiac valve defects caused by reduced enzyme activity during morphogenesis.
Significance: Screening these alleles could predict valve defects.

Cardiac valve defects are a common congenital heart malformation and a significant clinical problem. Defining molecular factors in cardiac valve development has facilitated identification of underlying causes of valve malformation. Gene disruption in zebrafish revealed a critical role for UDP-glucose dehydrogenase (UGDH) in valve development, so this gene was screened for polymorphisms in a patient population suffering from cardiac valve defects. Two genetic substitutions were identified and predicted to encode missense mutations of arginine 141 to cysteine and glutamate 416 to aspartate, respectively. Using a zebrafish model of defective heart valve formation caused by morpholino oligonucleotide knockdown of UGDH, transcripts encoding the UGDH R141C or E416D mutant enzymes were unable to restore cardiac valve formation and could only partially rescue cardiac edema. Characterization of the mutant recombinant enzymes purified from *Escherichia coli* revealed modest alterations in the enzymatic activity of the mutants and a significant reduction in the half-life of enzyme activity at 37 °C. This reduction in activity could be propagated to the wild-type enzyme in a 1:1 mixed reaction. Furthermore, the quaternary structure of both mutants, normally hexameric, was destabilized to favor the dimeric species, and the intrinsic thermal stability of the R141C mutant was highly compromised. The results are consistent with the reduced function of both missense mutations significantly reducing the ability of UGDH to provide precursors for cardiac cushion formation, which is essential to subsequent valve formation. The identification of these polymorphisms in patient populations will help identify families genetically at risk for valve defects.

Congenital heart defects, approximately one-fourth of which result from improper valve or septal formation (1), are a prevalent health concern (2). In many cases, the defects may be mild, and patients are not diagnosed until later in life, or the early defect is managed surgically but continues to require vigilant health awareness. Several genetic mutations have been correlated with these conditions (3, 4), but only a few of the molecular factors critical for normal heart development in humans have been well characterized.

Heart morphogenesis is a complex multistep process involving changes in expression of hundreds of different genes, as well as input from physical stimuli during development (3, 4). Model organisms such as zebrafish have been invaluable for delineation of important signaling molecules and receptors that modulate the necessary changes (5–8). In addition to specific signals, cell surface and extracellular adhesive molecules such as proteoglycans and glycosaminoglycans are essential for presentation of small molecules, local magnification of their potency, and generation of the hydrodynamic cushions ultimately needed for heart chamber and valve differentiation (3, 9, 10). The roles of genes involved in synthesis of these diverse anionic carbohydrate polymers have been defined by elegant genetic studies in which pre-cardial tissue from lethal disruptions is explanted and developmentally rescued with transduction of the targeted gene (9, 11).

UDP-glucose dehydrogenase (UGDH)[3] is one candidate gene essential for development in frogs (12), fruit flies (13),

* This work was supported, in whole or in part, by National Institutes of Health Grants CA106584 (to M. A. S.), R01 GM077289 (to J. J. B.), and NCRR P20 RR018759 (to M. A. S.). This work was also supported by American Heart Association Grant 0755788Z (to M. A. S., J. J. B., and J. B.).
[S] This article contains supplemental Fig. S1.
[1] To whom correspondence may be addressed: Cardiac Development and Genetics Group, Hubrecht Inst. for Developmental Biology and Stem Cell Research, Uppsalalaan 8, 3584 CT Utrecht, The Netherlands. Tel.: 31-30-212-1800; Fax: 31-30-251-6464; E-mail: j.bakkers@hubrecht.eu.
[2] To whom correspondence may be addressed: Dept. of Biochemistry, University of Nebraska, N246 Beadle Center, Lincoln, NE 68588-0664. Tel.: 402-472-9309; Fax: 402-472-7842; E-mail: msimpson2@unl.edu.

[3] The abbreviations used are: UGDH, UDP-glucose dehydrogenase; MO, morpholino; AV, atrioventricular; hpf, h post-fertilization.

nematodes (14), and mice (9, 15), shown in zebrafish to be critical specifically for cardiac valve formation (11). This enzyme produces UDP-glucuronate, key sugar nucleotide precursor for incorporation into the extracellular matrix glycosaminoglycan hyaluronan (16), modification of lipophilic hormones for enhanced solubilization and elimination (17), polymerization of heparan sulfate and chondroitin sulfate chains, as well as conversion to UDP-xylose to initiate proteoglycan production (10). Studies in bacterial (18, 19), plant (20, 21), bovine (22), and human (23) UGDH homologues show that all of them catalyze two successive oxidations of the 6′ carbon to orchestrate the same conversion of UDP-glucose to UDP-glucuronate (18–23). Notably, the enzyme is active in bacteria as a dimer (24), although in mammals and higher eukaryotes such as plant, nematode, fruit fly, and zebrafish, the enzyme purifies and functions as a hexamer (23, 25). This structure is a trimeric assembly of dimeric units (26), which are homologous to the bacterial dimer, organized in a toroidal formation that has been visualized by electron microscopy (25) and x-ray crystallography (see Fig. 1).

The structure has been solved for the human UGDH T131A apo form (Protein Data Bank code 3ITK), as a ternary complex with NAD^+ cofactor and UDP-glucuronate product (Protein Data Bank code 2QG4), as a ternary complex with NADH cofactor and UDP-glucose substrate (Protein Data Bank code 2Q3E) (27), and for UGDH E161Q as a thiohemiacetal between Cys-276 and the singly oxidized UDP-glucose, captured following the addition of NAD^+ and UDP-glucose (Protein Data Bank code 3KHU) (28). In a prior study, we used the human UGDH model to identify residues likely to be critical for catalytic activity and/or binding of the substrate and cofactor, which we subsequently confirmed using site-directed mutagenesis and enzymology (23, 29).

In a previously described large scale sequencing experiment using candidate genes essential for atrioventricular (AV) canal, AV septum, and AV valve formation, three patients with mitral valvar prolapse and mitral regurgitation were identified with novel missense mutations in the UGDH gene from among 192 patients with clinically diagnosed AV septal defects (30). Two of these individuals were heterozygous for a single nucleotide substitution that converted Arg-141 of UGDH to cysteine (R141C). A third individual was heterozygous for a mutation that converted Glu-416 to aspartate (E416D). Neither of these mutations was found in a control group of 350 normal individuals and inspection of sequence alignments showed that both residues are conserved in human, mouse, and zebrafish UGDH. Based on the UGDH model, the relevant residues were located unambiguously. Glu-416 is hydrogen-bonded to a water molecule that positions the UDP-glucose substrate (Fig. 1). Arg-141 is remote from the active site but relatively proximal to the putative subunit association faces of the enzyme.

In this report, the human UGDH polymorphisms and one additional mutation (I331N, also known as Jekyll (11)), previously noted to prevent cardiac valve development in zebrafish, were recreated in eukaryotic expression systems and in purified recombinant protein to determine the respective physiological and biochemical effects of the mutations. We examined the specific impact of UGDH mutants on AV valve development in zebrafish, the ability to rescue cardiac defects induced by the loss of UGDH, and compared these outcomes with the effect of mutations on steady state enzyme activity, quaternary structural assembly, and intrinsic stability of the protein. This comprehensive approach provided insights into the underlying molecular causes of valve defects in patients with UGDH polymorphisms and revealed novel aspects of UGDH enzymatic function.

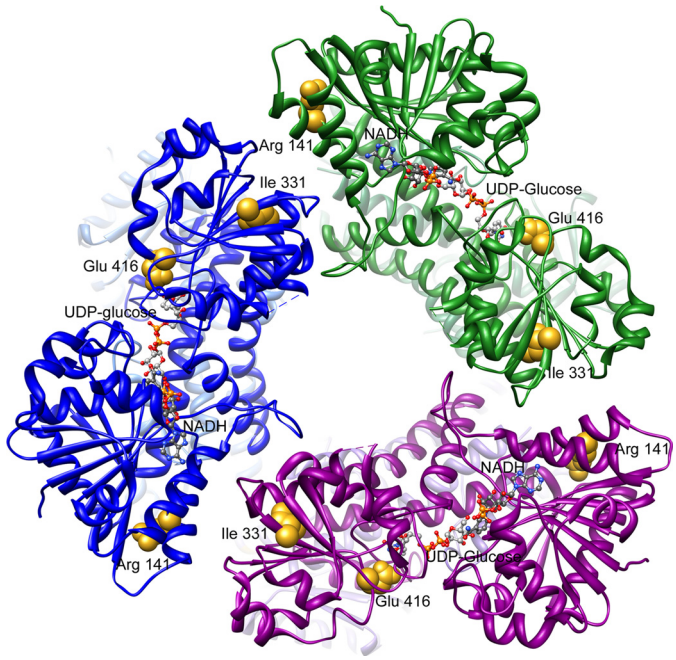

FIGURE 1. **Ribbon representation of UGDH and location of mutations characterized in this study.** The human hexameric enzyme is depicted from the top to illustrate the overall structure, the position of the active sites containing the substrate UDP-glucose, and the reduced cofactor NADH shown in ball and stick form, as well as residues Arg-141, Glu-416, and Ile-331, relative to the docking interface for association of the dimers to form a hexamer. Individual subunits are colored in dimeric pairs of *dark* and *light blue*, *dark* and *light green*, and *dark* and *light purple*. Amino acid side chains implicated in cardiac valve malformation are shown in space-filling form and colored *gold*.

EXPERIMENTAL PROCEDURES

In Situ Hybridization—Embryos were fixed in 4% formaldehyde, embedded in paraplast, and sectioned for *in situ* hybridization (10–14 μm). Labeled RNA probes were used to detect cardiac tropomyosin I or UGDH mRNA expression by *in situ* hybridization according to a previously described method (31). Representative images were digitally captured to illustrate message expression relative to AV canal and outflow tract.

Cardiac Valve Morphogenesis and in Vivo Rescue of Cardiac Edema in Zebrafish—Wild-type and transgenic (*Tg(Tie2:EGFP)*^{s849}) zebrafish were maintained under standard conditions (32). Two independent antisense morpholino oligonucleotides (MOs) were used to knock down *Ugdh* expression: *ugdh*-ATG MO, which was previously described (11), and *ugdh*-Splice MO (supplemental Fig. S1, 5′-AACAGCTCACACAAACACACCTGTA-3′). MOs were injected into embryos at the one cell stage (4 ng of *ugdh*-ATG MO or 2 ng of *ugdh*-Splice MO). Valve morphology was visualized by fluorescence microscopy on a Zeiss dissecting microscope. Representative digital images were captured at 48 h post-fertilization (hpf). For

cardiac phenotype rescue experiments, *in vitro* transcribed mRNA encoding UGDH wild type or R141C or E416D mutants was injected (10 μg/ml, 1 nl/embryo) concurrently with *Ugdh* MOs (4 ng/embryo) at the one-cell stage. Cardiac edema was evaluated and quantified at 55 hpf.

Hyaluronan Detection—To confirm functional Ugdh knockdown in embryos, we stained for hyaluronan on paraffin sections as described previously (33). Serum-free medium of HEK293 cells expressing a neurocan-alkaline phosphatase fusion protein was a generous gift from Uwe Rauch (University of Lund).

Generation and Purification of UGDH Point Mutants—Point mutants of human UGDH were generated from the wild-type constructs, UGDH-pET28a (for protein purification) or UGDH-pCS2 (for RNA injections in zebrafish), using the QuikChange site-directed mutagenesis kit (Stratagene, La Jolla, CA) according to the manufacturer's protocol. The sequences were verified by the Genomics Core at the University of Nebraska-Lincoln. Point mutants were expressed in *Escherichia coli* strain Rosetta2(DE3)pLysS (EMD Biosciences, Inc., San Diego, CA) and purified as N-terminal His_6 fusions as previously described (23). Following nickel affinity chromatography, the proteins were dialyzed against 0.1 M sodium phosphate, pH 7.4, and 1 mM DTT. All protein was stored at a concentration of 10 mg/ml.

Enzymatic Activity Measurement and Kinetic Characterizations—Activity of the point mutants was assayed by monitoring the change in absorbance at 340 nm that accompanies reduction of NAD^+ to NADH as reported previously (23). The R141C and E416D mutants exhibited saturable kinetics. Michaelis constants K_m and V_{max}, for UDP-glucose and NAD^+, were determined independently by holding [NAD^+] constant and varying [UDP-glucose] from 0 to 2 mM. Similarly, NAD^+ measurements were made by holding [UDP-glucose] constant and varying [NAD^+] from 0 to 2 mM. Specific activities were calculated from absorbance values using the molar extinction coefficient for NADH of 6220 M^{-1} cm^{-1}. Triplicate determinations for each concentration increment were plotted with PRISM (GraphPad Software, Inc., San Diego, CA). K_m and V_{max} were calculated by fitting the data to the Michaelis-Menten equation and assuming a single binding site/subunit for substrate and cofactor. Activity loss of wild-type and each mutant enzyme species was measured in aliquots removed at regular time points until no further activity was detectable. Each aliquot was assayed for 1 min with saturating cofactor and substrate. Specific activity was fitted to a semi-log plot following an initial lag period to calculate enzyme half-life. Statistical values were determined from these data by Student's unpaired two-tailed *t* test.

Molecular Mass Determination—Oligomeric state of the apo enzyme was determined by size exclusion chromatography as previously described (23). Each sample was precleared by centrifugation prior to loading. To determine the effect of substrate and cofactor inclusion on oligomeric state, purified recombinant UGDH wild type and point mutants were individually loaded on a Superdex 200 HR 10/300 column (GE Healthcare) using a 250-μl loop and separated by FPLC in 1× PBS in the presence of 1 mM UDP-glucose and 5 mM NAD^+ at a flow rate of 0.5 ml/min. Substrate and cofactor were included in each 250-μl load sample at the same final concentrations. Because of the interference from cofactor in UV absorbance readings from the column fractions of enzyme complexes, the protein content of these samples was measured at 595 nm upon the addition of Bradford reagent. The standards used were: thyroglobulin, 699 kDa; ferritin, 440 kDa; albumin, 67 kDa; β lactoglobulin, 35 kDa; and RNase A, 13.7 kDa. Resolution was sufficient to calculate molecular masses unambiguously in multiples of 57 kDa (the calculated molecular mass of monomeric His-tagged UGDH).

Protein Stability Determination—Purified recombinant UGDH wild type and point mutants were analyzed using a modified version of the Thermofluor stability assay as described by Ericsson *et al.* (34). Solutions of the wild-type and mutant apo enzymes (≈5 μg of protein in all cases, except I331N, which required 45 μg) were prepared in 1× PBS containing Sypro Orange dye (Invitrogen; 1:500 dilution). Samples containing substrate and cofactor were prepared in the same manner with UDP-glucose, and NAD^+ was added to a final concentration of 1 mM each. All samples were handled on ice throughout the preparation and transferred to an iCycler MyiQ Thermocycler (Bio-Rad) for analysis. The assay protocol was executed with the block initially cooled to 4 °C. After the addition of samples, the temperature was raised over a period of 76 min from 4 to 79 °C in 0.5 °C increments. The change in fluorescence was monitored for each sample at excitation and emission levels of 490 and 575 nm, respectively. Transitions representing the melting temperature, T_m, were obtained from the derivative of fluorescence with respect to temperature for at least 8–12 replicates and plotted as the means ± S.D.

RESULTS

Embryonic Localization of UGDH in the Developing Mouse Heart—It was previously shown that *ugdh* is required for heart valve formation in zebrafish embryogenesis (11) and is critical for gastrulation in mice, which arrest at embryonic day 9.5 when its function is disrupted (15). We first examined *Ugdh* distribution in mouse embryos, specifically to address its localization in cardiac development. At embryonic day 11.5, strong expression of *Ugdh* was observed in the endocardial cushions located within the AV canal (Fig. 2*A*). Both the endothelial cells covering the cushions and the mesenchymal cells within the cushions stained positive for *Ugdh* expression. At embryonic day 12.5, *Ugdh* mRNA was present in the endocardial cushions of the AV canal, in the dorsal mesenchymal protrusion and in the outflow tract cushions (Fig. 2, *B* and *C*). At E14.5, specific expression of *Ugdh* was observed in the valve leaflets located in the AV canal (Fig. 2*D*), which eventually become the leaflets of the mitral and tricuspid valves. *Ugdh* expression was not detectable in myocardium, which was visualized by staining for cardiac troponin I (*Tnni3*) (Fig. 2, *E–H*).

Functional Examination of UGDH R141C and E416D Variants in Zebrafish—To examine the effects of the single nucleotide polymorphisms identified in the candidate screen of congenital heart disease sufferers, we used a transgenic zebrafish model in which the endogenous expression of *Ugdh* was knocked down by antisense MO injection. In addition to a pre-

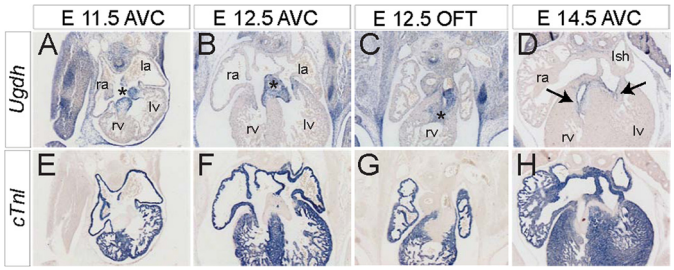

FIGURE 2. **Detection of *Ugdh* during mouse heart development illustrates localization of expression at sites of endocardial cushion formation preceding valve morphogenesis.** Mouse embryos at embryonic days 11.5, 12.5, and 14.5 were paraformaldehyde-fixed, agarose-embedded, and serially sectioned, followed by *in situ* hybridization with probes for *Ugdh* (*A–D*) and cardiac troponin I (cTnI, *E–H*). Representative light microscopic images are shown at the level of the atrioventricular canal (*AVC*; *A*, *B*, *D–F*, and *H*) or the cardiac outflow tract (*OFT*; *C* and *G*). *Asterisks* indicate the cushions in the AVC (*A* and *B*) or outflow tract (*C*). The *arrows* in *D* indicate the valve leaflets. *ra*, right atrium; *la*, left atrium; *rv*, right ventricle; *lv*, left ventricle; *lsh*, left sinus horn.

viously published *ugdh*-ATG MO, we designed and characterized a new *ugdh*-Splice MO that efficiently affected splicing of the endogenous *ugdh* mRNA (supplemental Fig. S1). To assess the functional consequence of *ugdh* MO injection on Ugdh activity in the embryo, we stained the embryos for hyaluronan, which is a key molecular fate for the UDP-glucuronate product of UGDH. We observed reduced hyaluronan accumulation in multiple tissues, including the heart, in embryos injected with the *ugdh* MOs relative to uninjected embryos (Fig. 3, *A* and *B*).

Next, we used a transgenic zebrafish line in which a GFP reporter is expressed under an endothelial cell-specific promoter (*Tg(Tie2:eGFP)*). Use of this model facilitates the visualization of cardiac valve defects because GFP-positive endothelial cells normally cluster in a ring at the AV boundary beginning at 43 hpf when valve formation initiates. As expected from previously reported data (11), injection of MOs targeting *ugdh* in zebrafish embryos at the single cell stage eliminated endocardial ring formation (Fig. 3, *C* and *D*). We were able to restore endocardial ring formation by coinjecting the *ugdh* MOs with mRNA encoding wild-type human UGDH (Fig. 3*E*). However, coinjection of UGDH R141C (Fig. 3*F*) or UGDH E416D (not shown) transcripts with the MOs failed to rescue the loss of endothelial clustering efficiently, suggesting that both polymorphisms conferred mutations to the UGDH enzyme that severely compromised its activity *in vivo*.

Embryos were further examined for cardiac morphogenesis as reflected in the presence of edema when the absence of endocardial ring formation failed to constrict the heart tube sufficiently for directional fluid flow. Cardiac edema was observed in >65% of embryos that had been injected with *ugdh* antisense MOs (Fig. 3*G*). Nearly all edema was eliminated by coinjection of wild-type human *UGDH* mRNA. However, consistent with the notion that functional defects are conferred by the UGDH R141C and E416D polymorphisms, coinjection of mRNA encoding either of these variants failed to rescue cardiac edema completely.

In Vitro Characterization of Purified UGDH R141C, E416D, and I331N (Jekyll)—To characterize the molecular defects in UGDH R141C and E416D variants more thoroughly and compare them with a previously reported defect, UGDH I331N,

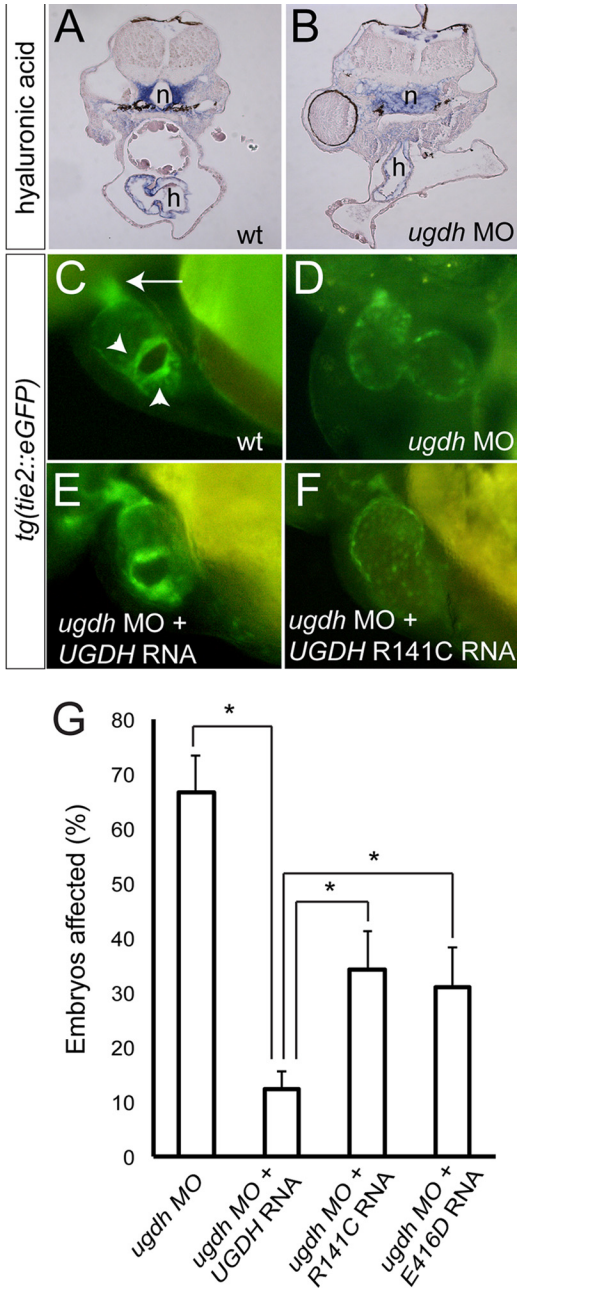

FIGURE 3. **Morphological defects in valve development and cardiac edema associated with UGDH deficiency are reversed by the addition of wild type but not mutant human *UGDH* transcripts.** *Tg(Tie2:EGFP)*^{s849} zebrafish were injected with control (wild type, *wt*) or antisense *Ugdh* MOs (*ugdh MO*, 4 ng) and imaged at 48 hpf on a fluorescence dissecting microscope. *A* and *B*, hyaluronan accumulation was visualized in embryonic sections from control (*A*) and MO-injected (*B*) fish with a specific hyaluronan-binding protein coupled to alkaline phosphatase. *n*, notochord; *h*, heart. *C–F*, images are focused on the AV boundary. The endocardial ring is clearly visible in wild-type (*arrowheads* in *C*) but not *ugdh* MO fish (*D*). Coinjection of wt *UGDH* mRNA with *ugdh* MO restored formation of the endocardial ring (*E*). However, coinjection of *ugdh* MO and UGDH mutant R141C did not rescue endocardial ring formation (*F*). *G*, zebrafish embryos were injected with *ugdh* MO at the single cell stage and were evaluated for cardiac edema at 48 hpf. As indicated, the ability of UGDH wt mRNA to rescue the cardiac morphogenesis defects inflicted by *ugdh* MO upon coinjection was assayed and compared with embryos coinjected with UGDH R141C or E416D mRNA (values ± S.E.). *, $p < 0.05$.

that prevented valve development in zebrafish, we generated and expressed each variant with an N-terminal six-histidine fusion for affinity purification as we have described (23, 29).

TABLE 1
Summary of wild-type and mutant UGDH kinetic constants

Enzyme	UDP-Glucose		NAD^+	
	V_{max}	K_m	V_{max}	K_m
	μmol/min/mg	*μM*	*μmol/min/mg*	*μM*
Wild-type	0.79 ± 0.02	9.19 ± 0.70	0.92 ± 0.02	415 ± 27
R141C	0.45 ± 0.01[a]	4.73 ± 0.24[c]	0.36 ± 0.01[a]	172 ± 23[c]
E416D	1.34 ± 0.01[a]	13.18 ± 0.42[c]	1.44 ± 0.03[a]	586 ± 31[c]
I331N	ND[b]	ND	ND	ND

[a] $p < 0.0001$ relative to wild type.
[b] ND, not detectable.
[c] $p < 0.001$ relative to wild type.

The constructs encoding UGDH R141C and E416D mutants expressed abundant soluble recombinant protein in *E. coli*, and each enzyme form was purified to homogeneity by nickel affinity chromatography. Typical yields were similar for wild type and both of these mutants, suggesting that neither mutation intrinsically reduced gene expression or solubility. However, the UGDH I331N construct yielded significantly reduced quantities of purified protein that was highly unstable even at 4 °C. Substrate dependence of the enzyme reaction converting UDP-glucose to UDP-glucuronate was not saturable for this mutant, which had minimal detectable activity. However, kinetics for the other two mutants were saturable, and these measurements were used to calculate Michaelis-Menten constants (summarized in Table 1). The R141C mutant V_{max} was only ≈40% of the maximum value for wild-type UGDH, which may partially explain its human phenotype but exhibited slightly lower K_m for both cofactor and substrate. In contrast, E416D had ≈40% higher V_{max} and moderately increased K_m values relative to the wild-type enzyme.

Half-life of Wild-type and Mutant UGDH—The differences in activity of the recombinant mutant enzymes were relatively nominal considering the magnitude of the phenotype conferred *in vivo* by a heterozygous mixture of wild-type and mutant UGDH enzyme species. Thus, we postulated that the effects on intrinsic activity could be mediated either by different conditions than those in which we assayed (*i.e.*, intracellular) and/or that the mutations influenced the stability of the functional enzyme. To test the latter point, we incubated UGDH wild type, R141C, and E416D individually at 37 °C and measured activity over time. The heterozygous condition was simulated in this experiment by pre-equilibrating a 1:1 mixture of wild-type UGDH with each mutant at 4 °C, followed by the activity time course at 37 °C.

UGDH R141C activity was, as expected, ≈40% of wild type at time 0 (not shown). To calculate the rate of activity loss independently of the initial value, activities at all time points were normalized to the 0-h average value (Fig. 4*A*). This mutant was highly unstable at 37 °C, with a $t_{½}$ of 10.5 ± 0.8 h, compared with the $t_{½}$ of 56.4 ± 6.2 h measured for the wild-type enzyme ($p = 0.005$). The results of this assay further showed that the mixture of wild type and R141C had a $t_{½}$ of 30.3 ± 2.6 h ($p = 0.009$ relative to wild type), intermediate between the activities measured in the pure protein solutions. Thus, the R141C mutant was capable of dramatically destabilizing activity of the wild-type enzyme in a physiologically relevant time frame.

UGDH E416D activity was, also as expected, slightly higher than wild type at time 0 (not shown), but it nonetheless lost activity somewhat more rapidly than wild type (Fig. 4*B*, $t_{½}$ = 41.8 ± 5.7 h, $p = 0.040$). The activity of the 1:1 mixture at 0 h, following its overnight incubation at 4 °C, was also diminished more rapidly. This suggests that the interaction of wild-type UGDH with E416D gave rise to an inactive protein population, with $t_{½}$ for the mixture of 37.8 ± 6.6 h ($p = 0.046$ relative to wild type).

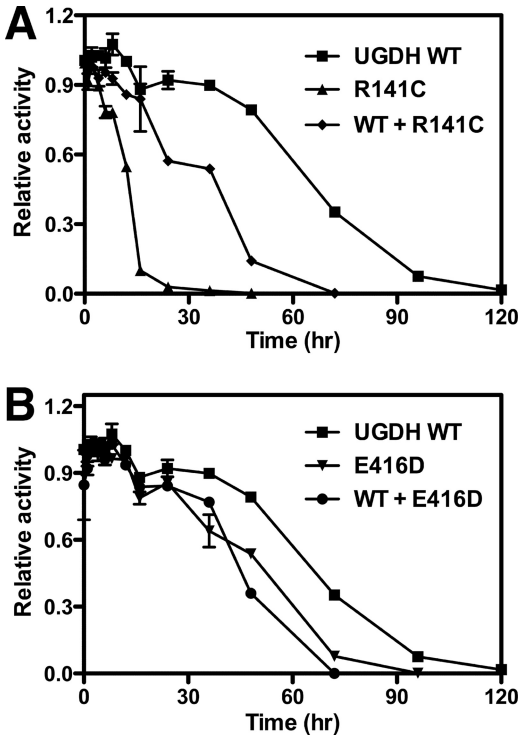

FIGURE 4. **Time-dependent activity of wild-type UGDH and point mutants.** Individual purified proteins or a 1:1 mixture of wild-type and mutant protein as indicated in the legend were equilibrated overnight at 4 °C. The samples were then placed at 37 °C. At the indicated time points, activity was assayed by the addition of the enzyme to phosphate buffer containing saturation concentrations of NAD^+ and UDP-glucose. The values plotted are the means ± S.D. for triplicate determinations. For several points, the *symbols* obscure the *error bars*. Absolute turnover was measured as the change in NADH absorbance at 340 nm in a 1-min assay for comparisons of wild type with R141C (*A*) or E416D (*B*). Absorbance values were normalized to the value at time 0 to illustrate the rate of activity loss.

Structural Integrity and Intrinsic Stability of Mutant UGDH—Our lab and others have previously shown that mammalian UGDH is active as a hexamer (23, 25, 35), and several of our previously characterized active site mutants show dissociation to an exclusively dimeric form with dramatic reduction in V_{max} or increased K_m. Therefore, we compared the quaternary structure of the R141C, E416D, and I331N mutants with that of wild-type UGDH by gel filtration chromatography. The wild-type protein eluted with peaks at molecular masses of ≈360 and ≈120 kDa, corresponding to a hexamer and a dimer, respectively, of the ≈57-kDa UGDH monomers (Fig. 5*A*, *solid black trace*), in which the hexamer was clearly the dominant peak. The elution profiles of both the E416D (Fig. 5*B*) and R141C (Fig. 5*C*) mutant enzymes were split in a hexamer-dimer equilibrium. In the case of E416D, the dimeric species accounted for ≈40% of the absorbance (≈60% dimer), whereas R141C appeared to be ≈80% dimeric. The I331N mutant was almost exclusively dimeric, with ≈10% of the absorbance attributable

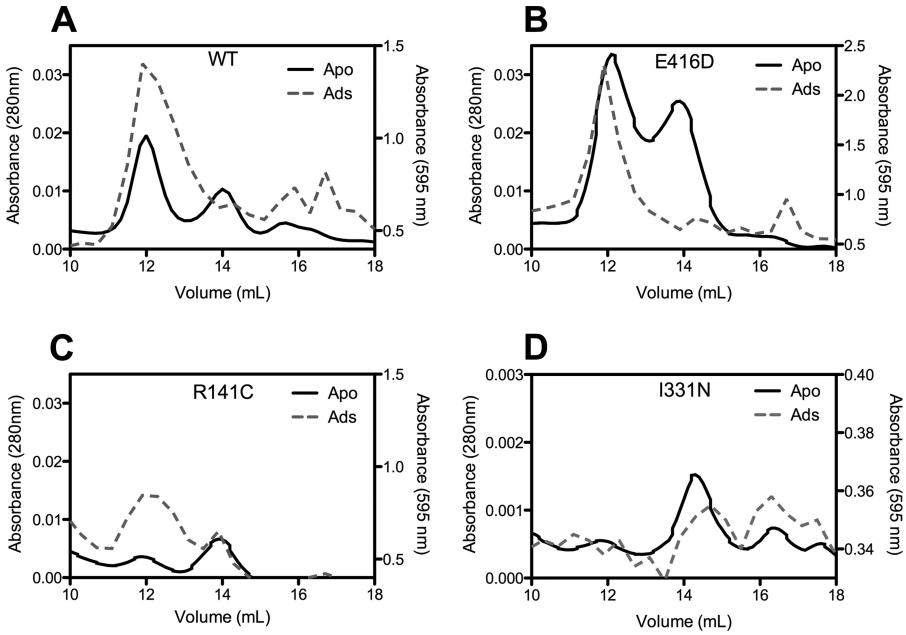

FIGURE 5. **Hexameric assembly of wild-type and mutant UGDH is sensitive to the presence of substrate and cofactor.** Purified wild-type and mutant UGDH was fractionated by gel filtration FPLC in the absence or presence of NAD^+ (5 mM) and UDP-glucose (1 mM). Absorbance was monitored at 280 and 595 nm, respectively. Size determination of each peak was made by comparison with molecular weight standards. Representative traces are plotted for wild-type UGDH (*A*), E416D (*B*), R141C (*C*), and I331N (*D*). On each plot, the apo-enzyme trace (in *black*) is superimposed on its holo-enzyme complement (in *gray*) for comparison of quaternary structure.

to a peak potentially corresponding to monomeric enzyme. Consistent with its previously noted instability, the total magnitude of the eluted peaks for I331N UGDH was reduced 10-fold relative to the wild type and other mutants (Fig. 5*D*).

Interestingly, including saturating levels of NAD^+ and UDP-glucose in the loaded protein and the column running buffer induced a complete shift of the wild-type UGDH elution profile to that of the hexamer (Fig. 5*A*, *dotted gray trace*). The same phenomenon was observed for the E416D mutant (Fig. 5*B*) and, to a lesser extent, the R141C mutant (Fig. 5*C*). Such a shift did not occur appreciably upon substrate and cofactor addition to I331N. Thus, it appeared that the formation of a holoenzyme ternary complex stabilized the hexameric quaternary assembly of the enzyme, and the extent of hexameric association was somewhat related to the level of stability of the wild type and each mutant as observed in the activity assays (Fig. 4).

To examine the intrinsic stability of UGDH and its point mutants in the presence and absence of its substrate and cofactor, we used a thermally sensitive fluorescence assay. Consistent with a previous report using this method (34), the observed melting temperature (T_m) was ≈50 °C for the apoenzyme form of wild-type UGDH and increased to ≈65 °C when NAD^+ and UDP-glucose were added to the reaction mixture (Table 2 and Fig. 6). Similar results were obtained for the E416D mutant. Although an increase in T_m with substrate and cofactor addition was observed for both of the other mutants as well, the apoenzyme form of the R141C mutant was denatured with a T_m several degrees lower than that of wild type, and the increase in T_m was only ≈8 °C. This effect was even more dramatic for the I331N mutant, which had a T_m of ≈40 °C for the apoenzyme and ≈46 °C for the ternary complex. These results are consistent with greater overall thermal stability of the hexameric form of UGDH and reflect the differences observed in the stability of the respective mutants.

TABLE 2

Summary of wild type and mutant UGDH melting temperatures

The ternary complex mixture includes 1 mM NAD^+ and 1 mM UDP-glucose.

Enzyme	T_m	
	Apo	Ternary
Wild-type	49.5 ± 0.3	64.8 ± 0.2
E416D	50.7 ± 0.2	63.5 ± 0.2
I331N	40.8 ± 2.7[a]	46.0 ± 1.4[b]
R141C	46.2 ± 1.0	55.0 ± 1.0[b]

[a] $p < 0.001$ relative to wild-type apoenzyme.
[a] $p < 0.001$ relative to wild-type holoenzyme.

DISCUSSION

UGDH is an enzyme that has been cloned and characterized from many diverse species and implicated in zebrafish heart development for over 10 years. To our knowledge, this is the first report of a characterization of mutations to UGDH occurring in a population of human patients with congenital heart valve defects. In this study, we localized expression of UGDH to a critical region of the developing mouse heart and followed its timed increase and subsequent decrease over the normal time frame for cardiac valve formation. We further demonstrated that the patient mutations R141C and E416D cannot rescue valve development or cardiac edema resulting from UGDH deletion in the zebrafish model. A detailed characterization of the structural and functional features of the mutant enzymes revealed modest alterations in the intrinsic activity of the enzyme that may translate to reduced function at cellular levels of substrate and cofactor. However, the most dramatic impact of the mutations on enzyme function appeared to derive from the striking destabilization of intrinsic thermal stability that leads to accelerated loss of activity in physiological conditions.

Importantly, we demonstrated that the presence of the mutant forms in a 1:1 ratio with wild-type UGDH, representative of the heterozygous genotype found in all patients with the polymorphisms, promotes a loss of wild-type UGDH activity as well.

UGDH was first identified as a cardiac valve initiation factor in zebrafish by isolating the gene disruption that was present in the zebrafish valve mutant *jekyll* (11). The lesion was found to be a single nucleotide substitution from A to T that generated an ATC to AAC codon change. The amino acid change, published as isoleucine to aspartate, is actually an isoleucine to asparagine mutation at a position that is highly conserved across numerous species including humans. The substitution had not been previously characterized in the context of the enzyme structure. We found the I331N mutant to be highly unstable and poorly expressed, with further impairment in quaternary structure assembly and virtually undetectable residual activity. These properties are a direct consequence of perturbations to the local environment of the Ile-331 residue by the substitution (Fig. 7*A*). This residue is located in a strongly hydrophobic core motif and is well packed among several other nonpolar amino acid side chains. Significant disruption to this stable, well conserved motif would be expected by the introduction of a hydrophilic amino acid side chain in any one of these positions, so this accounts for the strong effect of the asparagine substitution on UGDH stability.

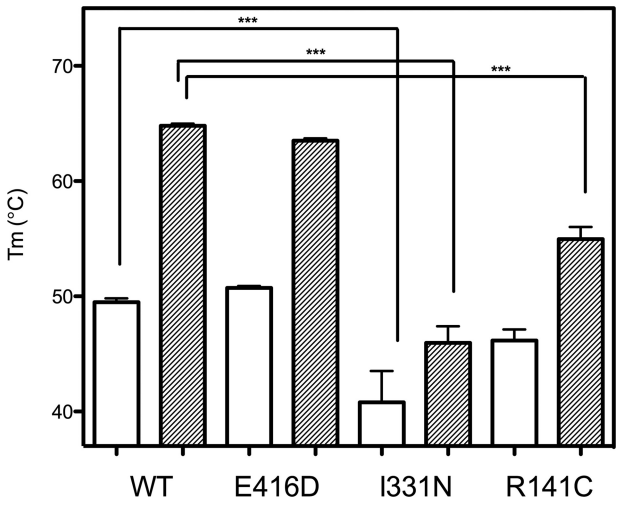

FIGURE 6. **UGDH is thermally stabilized by the addition of substrate and cofactor, but protein stability is compromised by mutations that occur at the dimer interface.** Purified wild-type UGDH and point mutants were thermally denatured in 0.5 °C increments from 4 to 79 °C in the presence of Sypro Orange. The change in fluorescence with respect to temperature was used to calculate a melting point (T_m) for each enzyme species in the absence (*white bars*) or presence (*gray bars*) of 1 mM UDP-glucose and 1 mM NAD^+. The means ± S.D. are plotted for the T_m of each enzyme. ***, $p < 0.001$; in addition, $p < 0.001$ for apo *versus* holo forms of wild-type, E416D, and R141C UGDH.

Examination of Glu-416 in the context of the UGDH ternary complex structure (Fig. 7*B*) illustrates its role in indirect positioning of the UDP-glucose substrate via two water molecules in collaboration with the side chain of lysine 339. The backbone of the loop containing Lys-339 is stabilized by hydrogen bonding to Glu-416. Thus, effects of the E416D substitution were predicted to include decreased binding of UDP-glucose. In fact, the K_m for UDP-glucose is increased by ≈50% (Table 1). This relatively modest reduction in apparent affinity for substrate in the context of enzymatic turnover is also accompanied by a significant acceleration in the loss of activity at 37 °C (Fig. 4) and destabilization of the hexameric quaternary assembly in the absence of substrate and cofactor (Fig. 5), although the intrinsic thermal stability is not compromised (Fig. 6). We previously found that the K339A substitution increased K_m for UDP-glucose by >150-fold, and yielded an exclusively dimeric apoenzyme. The more direct role in UDP-glucose coordination through interaction with both phosphate groups accounts for the significant difference in K_m between the K339A and E416D mutants. The observed effect on the hexamer-dimer equilibrium is consistent with a link between active site integrity, substrate and cofactor binding capacity, and hexameric assembly, which ultimately determines enzyme stability. Reduced stabil-

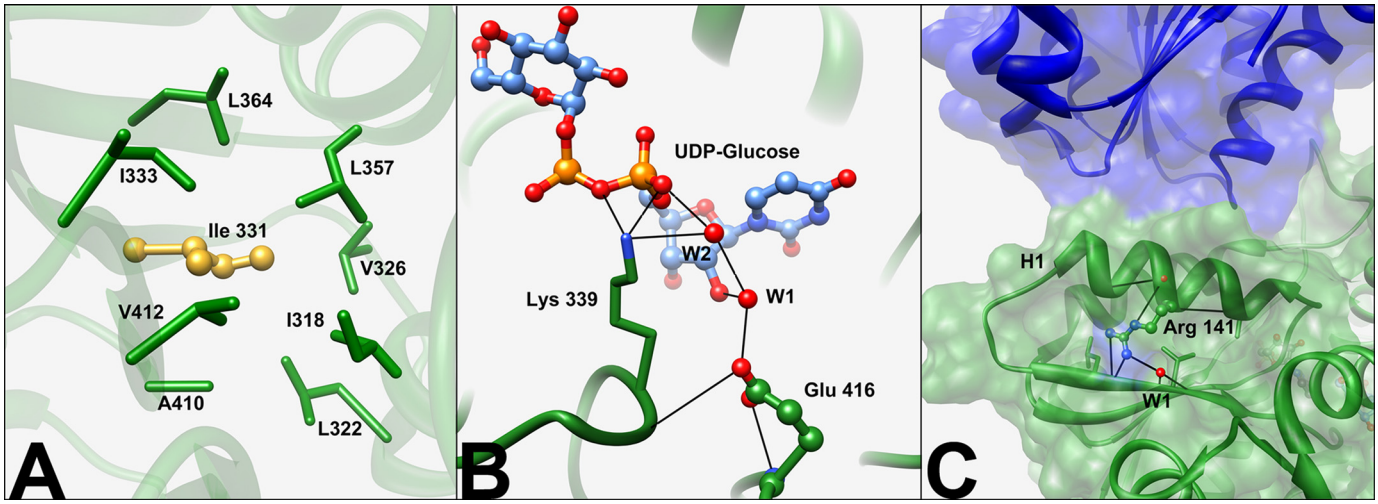

FIGURE 7. **Local interactions in UGDH near sites of clinically relevant mutations.** *A*, the core of UGDH is depicted transparently with key hydrophobic residues shown as wires. Ile-331 is shown in ball and stick conformation colored *gold*. *B*, the substrate UDP-glucose is represented in ball and stick form colored by heteroatom. Glu-416 is also represented as ball and stick directly hydrogen-bonded (*black lines*) to a water (*W1*) and the backbone of a loop. Glu-416 is involved in positioning UDP-glucose in its binding pocket by coordinating two waters (*W1* and *W2*) and Lys-339, depicted in wire form. *C*, surface filling model of the dimer interface is shown in *green* and *blue*. Each dimer pair is colored a separate color such that the interface is between two dimers. Arg-141 is represented in ball and stick form hydrogen-bonded (*black lines*) to a water (*W1*) as well as the backbone of helix 1 (*H1*).

ity of the E416D hexamer results in propagation of instability to the wild-type enzyme, as observed in a simulated heterozygous condition (Fig. 4), so this is a likely explanation for the effects of this mutation on cardiac valve morphogenesis, as discussed below.

Comparison of results from the R141C mutant is consistent with this explanation. Arg-141 is located at the interface between dimeric units of the hexamer (Fig. 1) and maintains a hydrogen bond network that stabilizes a helix-loop-β motif critical to the dimer-dimer association (Fig. 7*C*). Substitution of this residue with a cysteine eliminates these contacts and releases the helix from its tight association, which would be expected to disrupt the quaternary structure to an exclusively dimeric form as was shown in Fig. 5. The reduced stability of the dimer is associated with a reduction in enzymatic activity (Table 1), destabilization of the mutant in both a homozygous and a heterozygous reaction mixture (Fig. 4), and significantly reduced thermal stability in the absence or presence of ternary complex components (Fig. 6). The reductions in activity and stability are probable underlying causes of the phenotype associated with this missense mutation in human patients.

The relatively modest differences in enzymatic activity of the R141C and E416D mutants is not entirely surprising because bacterial homologues are only found as dimers (24). However, the inability to form normal complexes may nonetheless have dramatic impact on the stability of wild-type heterohexamers with either R141C or E416D and/or on the potential for allosteric regulation within a cellular context. This is particularly intriguing because the addition of substrate and cofactor at saturating levels can fully restore the hexameric structure. Although hexameric structure is not critical for achieving wild-type maximum reaction velocity if optimal conditions are provided (29), studies of the nucleotide sugar dehydrogenase family member GDP-mannose dehydrogenase (36) suggest that hexameric structure provides the capacity for allosteric regulation and cooperativity with respect to substrate use. Thus, the effects on quaternary assembly, particularly the ability to restore and maintain a stable ternary complex within a physiological range of available substrate and cofactor, could translate to significant differences in the net enzymatic activity in developmentally critical phases.

UGDH is the only enzyme that provides UDP-glucuronate, which is an essential precursor for hyaluronan synthesis, initiation of all proteoglycan synthesis, and elongation of the glycosaminoglycan chains that comprise proteoglycans. In mice, UGDH gene disruption is embryonically lethal (15), and in zebrafish Ugdh inactivation results in cardiac valve defects (11). UGDH and HAS2 gene disruption have identical phenotypes, and cardiac tissue explant studies, in which AV septum formation can be restored by exogenous hyaluronan, the product of the HAS2 gene, demonstrate that UGDH must function at a high level during heart formation to supply precursors for hyaluronan production (9). It has been further shown in the *Xenopus* model system that UGDH expression directly dictates the production capacity for hyaluronan during development (12). Our results show that UGDH is expressed at a very high level specifically in the region of the developing valves throughout valve development (Fig. 2). The introduction of transcripts encoding either the R141C or E416D mutant form of UGDH was insufficient to support valve formation or prevent cardiac edema (Fig. 3), which clearly illustrates a significant level of impairment resulting from these missense mutations *in vivo*.

Based on the infrequency with which UGDH mutations have been reported, it is likely that most UGDH polymorphisms do not yield viable embryos. In support of the extreme phenotypic distress conferred by such lesions, only the heterozygous and not the homozygous expression of R141C and E416D is observed in the population study (30). The characterizations we described above point toward a significant loss of enzyme stability and resultant reduction in UDP-glucuronate production below the levels that are required to sustain hyaluronan synthesis while the cardiac cushions are forming. Cardiac cushions are largely the result of rapid hyaluronan extrusion and accumulation between the layers of the myocardium and endocardium beginning at embryonic day 9.5. Their formation produces tissue protrusions that are invaded by endocardial cells, which delaminate because of epithelial to mesenchymal transition. Their absence prevents epithelial to mesenchymal transition for cell migration into the AV septum, which is needed for subsequent valve differentiation. Because this process necessitates rapid deposition of large quantities of hyaluronan, UGDH function is critical at this time, and even modest reductions in its function are clearly disruptive. Screening families for these alleles may assist in the prediction of cardiac valve defects and offer therapeutic targets.

REFERENCES

1. Hoffman, J. I., and Kaplan, S. (2002) The incidence of congenital heart disease. *J. Am. Coll. Cardiol.* **39,** 1890–1900
2. Hoffman, J. I., Kaplan, S., and Liberthson, R. R. (2004) Prevalence of congenital heart disease. *Am. Heart J.* **147,** 425–439
3. Armstrong, E. J., and Bischoff, J. (2004) Heart valve development. Endothelial cell signaling and differentiation. *Circ. Res.* **95,** 459–470
4. Bartman, T., and Hove, J. (2005) Mechanics and function in heart morphogenesis. *Dev. Dyn.* **233,** 373–381
5. Fishman, M. C., and Stainier, D. Y. (1994) Cardiovascular development. Prospects for a genetic approach. *Circ. Res.* **74,** 757–763
6. Gelb, B. D. (1997) Molecular genetics of congenital heart disease. *Curr. Opin. Cardiol.* **12,** 321–328
7. Warren, K. S., and Fishman, M. C. (1998) "Physiological genomics." Mutant screens in zebrafish. *Am. J. Physiol.* **275,** H1–H7
8. Yelon, D., and Stainier, D. Y. (1999) Patterning during organogenesis. Genetic analysis of cardiac chamber formation. *Semin. Cell Dev. Biol.* **10,** 93–98
9. Camenisch, T. D., Spicer, A. P., Brehm-Gibson, T., Biesterfeldt, J., Augustine, M. L., Calabro, A., Jr., Kubalak, S., Klewer, S. E., and McDonald, J. A. (2000) Disruption of hyaluronan synthase-2 abrogates normal cardiac morphogenesis and hyaluronan-mediated transformation of epithelium to mesenchyme. *J. Clin. Invest.* **106,** 349–360
10. Prydz, K., and Dalen, K. T. (2000) Synthesis and sorting of proteoglycans. *J. Cell Sci.* **113,** 193–205
11. Walsh, E. C., and Stainier, D. Y. (2001) UDP-glucose dehydrogenase required for cardiac valve formation in zebrafish. *Science* **293,** 1670–1673
12. Vigetti, D., Ori, M., Viola, M., Genasetti, A., Karousou, E., Rizzi, M., Pallotti, F., Nardi, I., Hascall, V. C., De Luca, G., and Passi, A. (2006) Molecular cloning and characterization of UDP-glucose dehydrogenase from the amphibian *Xenopus laevis* and its involvement in hyaluronan synthesis. *J. Biol. Chem.* **281,** 8254–8263
13. Häcker, U., Lin, X., and Perrimon, N. (1997) The *Drosophila* sugarless gene modulates Wingless signaling and encodes an enzyme involved in polysaccharide biosynthesis. *Development* **124,** 3565–3573

14. Hwang, H. Y., and Horvitz, H. R. (2002) The *Caenorhabditis elegans* vulval morphogenesis gene *sqv-4* encodes a UDP-glucose dehydrogenase that is temporally and spatially regulated. *Proc. Natl. Acad. Sci. U.S.A.* **99,** 14224–14229
15. García-García, M. J., and Anderson, K. V. (2003) Essential role of glycosaminoglycans in Fgf signaling during mouse gastrulation. *Cell* **114,** 727–737
16. Fraser, J. R., Laurent, T. C., and Laurent, U. B. (1997) Hyaluronan. Its nature, distribution, functions and turnover. *J. Intern. Med.* **242,** 27–33
17. Tukey, R. H., and Strassburg, C. P. (2000) Human UDP-glucuronosyltransferases. Metabolism, expression, and disease. *Annu. Rev. Pharmacol. Toxicol.* **40,** 581–616
18. Campbell, R. E., Sala, R. F., van de Rijn, I., and Tanner, M. E. (1997) Properties and kinetic analysis of UDP-glucose dehydrogenase from group A streptococci. Irreversible inhibition by UDP-chloroacetol. *J. Biol. Chem.* **272,** 3416–3422
19. Ge, X., Penney, L. C., van de Rijn, I., and Tanner, M. E. (2004) Active site residues and mechanism of UDP-glucose dehydrogenase. *Eur. J. Biochem.* **271,** 14–22
20. Stewart, D. C., and Copeland, L. (1998) Uridine 5′- diphosphate-glucose dehydrogenase from soybean nodules. *Plant Physiol.* **116,** 349–355
21. Turner, W., and Botha, F. C. (2002) Purification and kinetic properties of UDP-glucose dehydrogenase from sugarcane. *Arch. Biochem. Biophys.* **407,** 209–216
22. Schiller, J. G., Bowser, A. M., and Feingold, D. S. (1972) Studies on the mechanism of action of UDP-D-glucose dehydrogenase from beef liver. II. *Carbohydr. Res.* **25,** 403–410
23. Sommer, B. J., Barycki, J. J., and Simpson, M. A. (2004) Characterization of human UDP-glucose dehydrogenase. CYS-276 is required for the second of two successive oxidations. *J. Biol. Chem.* **279,** 23590–23596
24. Campbell, R. E., Mosimann, S. C., van De Rijn, I., Tanner, M. E., and Strynadka, N. C. (2000) The first structure of UDP-glucose dehydrogenase reveals the catalytic residues necessary for the two-fold oxidation. *Biochemistry* **39,** 7012–7023
25. Franzen, J. S., Ashcom, J., Marchetti, P., Cardamone, J. J., Jr., and Feingold, D. S. (1980) Induced versus pre-existing asymmetry models for the half-of-the-sites reactivity effect in bovine liver uridine diphosphoglucose dehydrogenase. *Biochim. Biophys. Acta* **614,** 242–255
26. Spicer, A. P., Kaback, L. A., Smith, T. J., and Seldin, M. F. (1998) Molecular cloning and characterization of the human and mouse UDP-glucose dehydrogenase genes. *J. Biol. Chem.* **273,** 25117–25124
27. Egger, S., Chaikuad, A., Kavanagh, K. L., Oppermann, U., and Nidetzky, B. (2011) Structure and mechanism of human UDP-glucose 6-dehydrogenase. *J. Biol. Chem.* **286,** 23877–23887
28. Egger, S., Chaikuad, A., Klimacek, M., Kavanagh, K. L., Oppermann, U., and Nidetzky, B. (2012) Structural and kinetic evidence that catalytic reaction of human UDP-glucose 6-dehydrogenase involves covalent thiohemiacetal and thioester enzyme intermediates. *J. Biol. Chem.* **287,** 2119–2129
29. Easley, K. E., Sommer, B. J., Boanca, G., Barycki, J. J., and Simpson, M. A. (2007) Characterization of human UDP-glucose dehydrogenase reveals critical catalytic roles for lysine 220 and aspartate 280. *Biochemistry* **46,** 369–378
30. Smith, K. A., Joziasse, I. C., Chocron, S., van Dinther, M., Guryev, V., Verhoeven, M. C., Rehmann, H., van der Smagt, J. J., Doevendans, P. A., Cuppen, E., Mulder, B. J., Ten Dijke, P., and Bakkers, J. (2009) Dominant-negative ALK2 allele associates with congenital heart defects. *Circulation* **119,** 3062–3069
31. Moorman, A. F., Houweling, A. C., de Boer, P. A., and Christoffels, V. M. (2001) Sensitive nonradioactive detection of mRNA in tissue sections. Novel application of the whole-mount *in situ* hybridization protocol. *J. Histochem. Cytochem.* **49,** 1–8
32. Westerfield, M. (2007) *The Zebrafish Book: A Guide for the Laboratory Use of Zebrafish (Danio rerio)*, 5th Ed., University of Oregon Press, Eugene, OR
33. Bakkers, J., Kramer, C., Pothof, J., Quaedvlieg, N. E., Spaink, H. P., and Hammerschmidt, M. (2004) Has2 is required upstream of Rac1 to govern dorsal migration of lateral cells during zebrafish gastrulation. *Development* **131,** 525–537
34. Ericsson, U. B., Hallberg, B. M., Detitta, G. T., Dekker, N., and Nordlund, P. (2006) Thermofluor-based high-throughput stability optimization of proteins for structural studies. *Anal. Biochem.* **357,** 289–298
35. Franzen, J. S., Ishman, R., and Feingold, D. S. (1976) Half-of-the-sites reactivity of bovine liver uridine diphosphoglucose dehydrogenase toward iodoacetate and iodoacetamide. *Biochemistry* **15,** 5665–5671
36. Naught, L. E., Gilbert, S., Imhoff, R., Snook, C., Beamer, L., and Tipton, P. (2002) Allosterism and cooperativity in *Pseudomonas aeruginosa* GDP-mannose dehydrogenase. *Biochemistry* **41,** 9637–9645

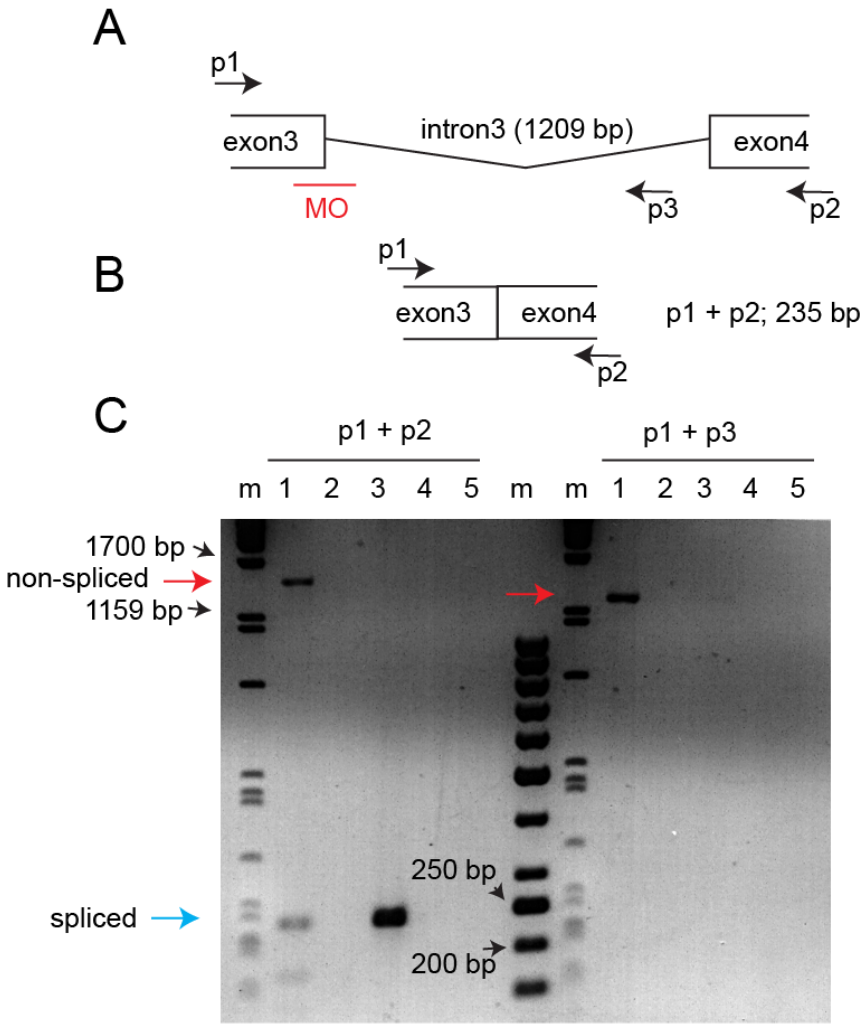

m; marker
1; ugdh-splice MO
2; ugdh-splice MO -RT
3; uninjected control
4; uninjected control -RT
5; water

Supplementary Figure 1. Injection of ugdh splice-MO affects endogenous ugdh mRNA spicing.
(A) Schematic presentation of genomic ugdh region around exon 3 and 4. The ugdh splice-MO targets the proposed splice donor site of exon 3 (red line). Position of PCR primers are indicated by arrows. (B) Schematic presentation when correct splicing has occurred. Primers p1 and p2 will generate a 235 base pair (bp) PCR fragment. (C) Agarose gel showing PCR fragments after reverse transcriptase using primer combinations indicated. Reverse transcriptase (RT) PCR was performed on RNA isolated from 2 day old embryos uninjected or injected with the ugdh splice MO. –RT, negative control without reverse transcriptase; red arrow, unspliced PCR fragment; blue arrow, correct spliced PCR fragment.